Shallow shear-wave velocity structure of Solfatara volcano (Campi Flegrei, Italy), from inversion of Rayleigh-wave dispersion curves

S. Petrosino, P. Cusano and G. Saccorotti

Istituto Nazionale di Geofisica e Vulcanologia – Osservatorio Vesuviano – Napoli, Italy

(Received May 16, 2005; accepted March 10, 2006)

ABSTRACT In this work, we infer the 1D shear-wave velocity model at Solfatara volcano using the dispersion properties of Rayleigh waves generated by artificial explosions. The group-velocity dispersion curves are retrieved by applying the Multiple Filter Technique to single-station recordings of air-gun sea shots. Seismic signals are filtered in different frequency bands and the dispersion curves are obtained by evaluating the arrival times of the envelope maxima of the filtered signals. Fundamental and higher modes are carefully recognized and separated by using a Phase Matched Filter. The dispersion curves obtained indicate Rayleigh-wave fundamental-mode group velocities ranging from about 0.8 to 0.6 km/s over the 2-12 Hz frequency band. These group velocity dispersion curves are then inverted to infer a shallow shear-wave velocity model down to a depth of about 250 m. The shear-wave velocities thus obtained are compatible with those derived both from cross- and down-hole measurements in neighbouring wells and from laboratory experiments. These data are eventually interpreted in the light of the geological setting of the area. Using the velocity model obtained, we calculate the theoretical ground response to a vertically-incident S-wave getting two, main amplification peaks centered at frequencies of 2.2 and 5.4 Hz. The transfer function was compared to those obtained experimentally from the application of Nakamura's technique to microtremor data, artificial explosions and local earthquakes. Agreement among the experimental and theoretical transfer functions is observed for the amplification peak of frequency 5.4 Hz.

Introduction

It is well known that shallow layers with high impedance contrasts affects the ground motion, causing strong amplifications (Bard and Bouchon, 1980; Hough *et al*., 1990). Therefore, the detailed knowledge of the velocity structure at shallow depths is of great relevance for the quantitative estimate of the theoretical ground response to a seismic input. Such determinations are crucial especially in densely urbanized areas, where a quantitative assessment of the amplification factors is necessary for a correct evaluation of seismic hazard.

Moreover, a reliable determination of the velocity model is also particularly important for seismic source studies in volcanic areas, where the presence of highly heterogeneous and/or fractured materials can lead to anomalous propagation and site effects that could mask the contribution of the source in the seismic signals.

In the last years, the determination of the seismic velocities at shallow depths from the

dispersion of surface waves has become increasingly popular. Single-station (MFT: Herrmann, 1973, 1987) and multichannel (MASW, SPAC: Aki, 1957; Louie, 2001; Bettig *et al*., 2001) techniques have been used with the aim of obtaining the group and phase velocity dispersion curves and inferring the shallow velocity structure in both sedimentary and volcanic areas (Malagnini *et al*., 1995; Petrosino *et al*., 2002; Saccorotti *et al*., 2003). This information has often been used to estimate the theoretical transfer function and hence to assess the site effects (Malagnini *et al*., 1996).

In this work, we apply the single station Multiple Filter Technique (MTF) to the seismic signals generated by air-gun shots to retrieve the Rayleigh wave dispersion properties in the Solfatara volcanic area. From the inversion of the dispersion curves, we infer the 1D velocity model down to a depth of 250 m, and use this model to calculate the theoretical ground response to a vertically incident S-wave. Eventually, Nakamura's technique (Nakamura, 1989) is applied to seismic noise in order to compare the experimental H/V spectral ratio with the theoretical transfer function.

Geological setting

The Campi Flegrei is a nested caldera originated by two large collapses that occurred during the Campanian Ignimbrite (39 ka) and the Neapolitan Yellow Tuff (NYT, 15 ka) eruptions [see Orsi *et al*. (1996, 2003); Di Vito *et al*. (1999) for a detailed description of the volcanological evolution]. Since 15 ka ago the volcanic activity concentrated inside the NYT caldera and many eruptions took place during three distinct epochs of activity, alternated with two periods of quiescence. In particular, volcanism of the I epoch (15-9.5 ka) includes variable magnitude explosive eruptions. During this epoch several tuff-cones were formed near the present coast of Pozzuoli (Rione Terra, La Pietra).

During the II epoch (8.6-8.2 ka), the volcanic activity occurred along the north-eastern structural boundary of the NYT caldera, whereas vents (Solfatara, Accademia, Monte Olibano) of the III epoch (4.8-3.8 ka) were mainly located in the north-eastern sector of the caldera floor, near the present town of Pozzuoli.

Since the NYT collapse, the whole Campi Flegrei caldera is affected by subsidence, while the younger, central part of the caldera floor is characterized by resurgence. During the three epochs of volcanic activity, the La Starza marine terrace (the most uplifted part of the resurgent block) alternated periods of emersion and submersion and after the onset of the III epoch it definitely emerged.

The stratigraphic, structural and geochronological observations have widely contributed to define this complex volcanological evolution. For example, evidence of the eruptive activity of the I and III epoch and the sequence of La Starza comes from the stratigraphic data and borehole drillings in the area of Pozzuoli that show the presence of tuff rocks overlaid by pyroclastic and marine deposit layers of variable thickness. This data were also used to trace a possible geological section across the town of Pozzuoli, moving from the shore (Rione Terra) towards the Solfatara, along a NNE-SSW profile (Lirer *et al*., 1987).

Data analysis

For the dispersion analysis of Rayleigh waves, we used seismic signals produced by air-gun sea shots, fired in the Gulf of Pozzuoli on September 2001 during the active seismic experiment "Serapis" (Zollo *et al*., 2003). These signals were recorded by SLF and SFT stations of the Osservatorio Vesuviano seismic network, located in the Solfatara crater (Fig. 1), at an inter-station distance of about 160 m.

The SLF Mars Lite digital seismic station was equipped with a three-component 1-Hz LE3DLITE geophone. The SFT analogic station was equipped with a L4-3D Mark Products seismometer with natural frequency of 1 Hz. The sampling rate was 125 and 100 sps for stations SLF and SFT, respectively. Examples of recordings are shown in Figs. 2 and 3.

From the whole data set, consisting of about 5000 shots, we selected 36 recordings associated with source-receiver distances ranging from 2.5 to 4.0 km and high signal-to-noise ratios. We obtained preliminary group velocity dispersion curves applying the MFT (Dziewonski *et al*., 1969; Herrmann, 1973) to the vertical-component seismograms recorded by station SLF. We cut the signals by taking 2048 samples starting from the P-wave onset, then each seismogram was bandpass filtered for a set of center frequencies spanning the 1-12 Hz frequency range with a 0.2 Hz step; the bandwidth of the Gaussian filter was set equal to a half of the center frequency. The occurrence time of the envelope maximum of the filtered signal was used to calculate the group velocity at each frequency. For each shot, the MFT produces a plot (hereinafter referred to as MF plot; see examples in Figs. 2 and 3) of the contoured normalized envelope amplitude as a

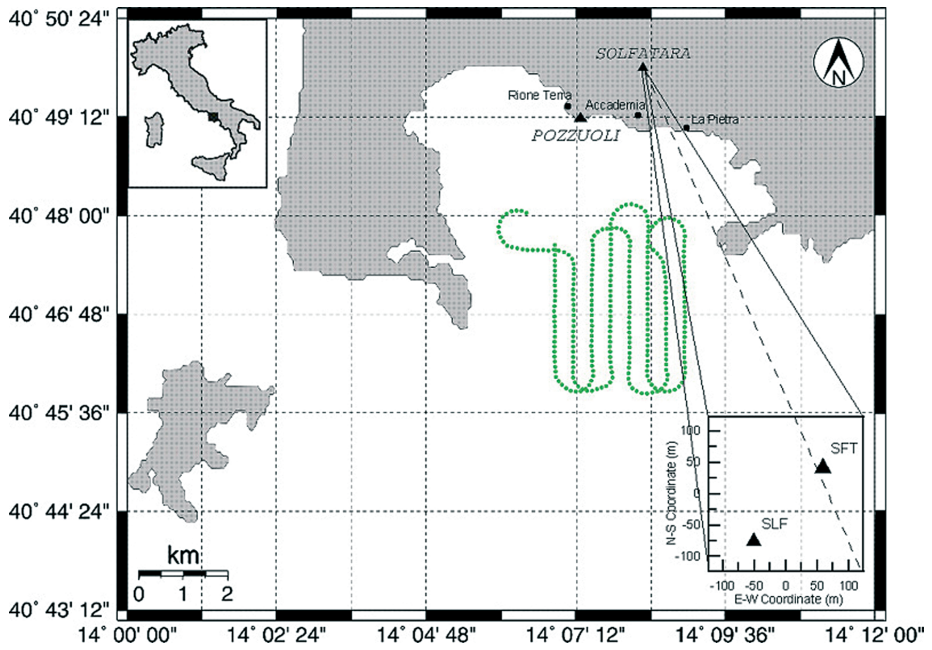

Fig. 1 - Map of the Campi Flegrei area and location of the seismic stations (triangle). Dots represent the location of the air-gun shots fired on September 21, 2001.

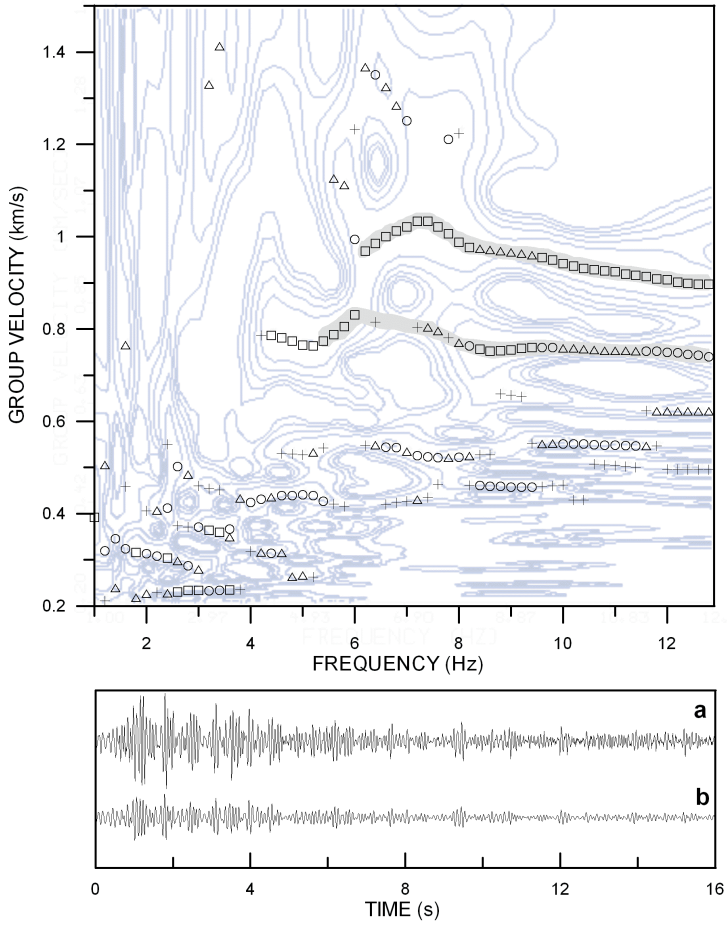

Fig. 2 - In the upper panel: result of MFT analysis applied to a shot recorded at the station SLF. Contour lines depict the amplitude of the signal envelope. Symbols represent the four largest maxima of the envelope at each frequency: from the largest maxima to the smallest ones, the symbols used are squares, circles, triangles, and crosses. First and second higher mode dispersion associated to the continuous sequence of the envelope maxima is evidenced by the grey-shaded area. In the lower panel: a) vertical component seismogram; b) filtered signal in the 1-12 Hz band.

function of frequency and group velocity. In these plots, for each spot frequency the four largest envelope maxima are marked by a symbol. The group velocity dispersion curve can be extracted by picking the adjacent symbol that depicts a continuous pattern.

A great problem in surface wave analysis of multiple-modal signals is the contamination of the higher modes that could mask the real dispersive patterns and false the picking of the dispersion curves. To avoid this problem, the signals need to be filtered by using a Phase Matched Filter (PMF; Herrin and Goforth, 1977). This filter, that allows the separation of different modes, requires the estimate of a trial, approximate dispersion curve that will be refined at the end of the filtering iterative procedure.

To apply the PMF to our data set, we have to select the trial dispersions, so we very carefully visually inspected the MF plots associated to the recordings of station SLF and searched for clear and well-separated dispersion curves. The dispersion curve of the first higher mode was always very clear for every analysed shot, with group velocities ranging from ~820 m/s to ~740 m/s in the 6-12 Hz frequency band. For a great number of MF plots, we could also identify the second higher mode, while the fundamental mode sometimes appeared contaminated by the higher modes and did not show a clear dispersive pattern (see Fig. 2 where the fundamental mode seems to have a double branch), so we decided not to pick it at this station. Conversely, we were able to successfully pick a clear fundamental mode dispersion curve from the MF plots associated with recordings from station SFT (Fig. 3).

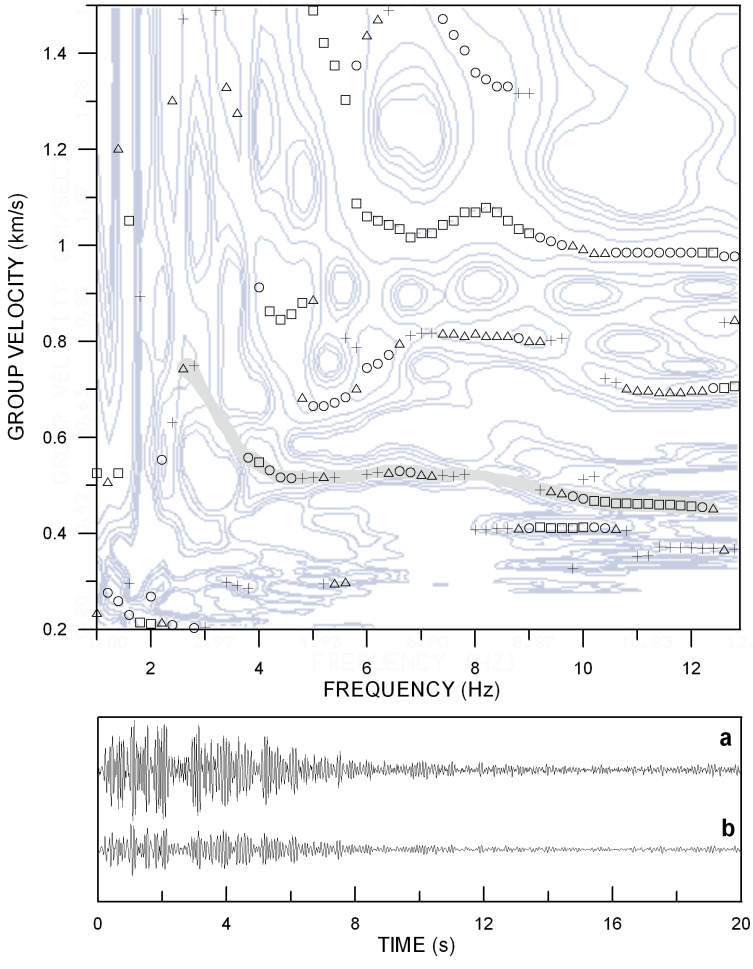

Fig. 3 - In the upper panel: result of MFT analysis applied to a shot recorded at SFT stations. See the caption of Fig. 2 for the description of the symbols. Fundamental mode dispersion associated to the continuous sequence of the envelope maxima is evidenced by the grey-shaded area. In the lower panel: a) vertical component seismogram; b) filtered signal in the 1-12 Hz band.

The fundamental mode and two higher-mode dispersions previously derived were used as trial curves for the PMF, which was first applied to the signals from the SLF station. This procedure is summarized in the following steps:

1. the 36 waveforms were filtered by using the trial curve of the first higher mode to allow the separation of the first-mode wave-packet from the residual seismograms;
2. the residual seismograms were filtered by using the trial curve of the second higher mode, to separate the second-mode wave-packet from the new residual seismograms;
3. the new residual waveforms were filtered by using the trial curve of the fundamental mode, to extract the "fundamental-mode wave-packet".

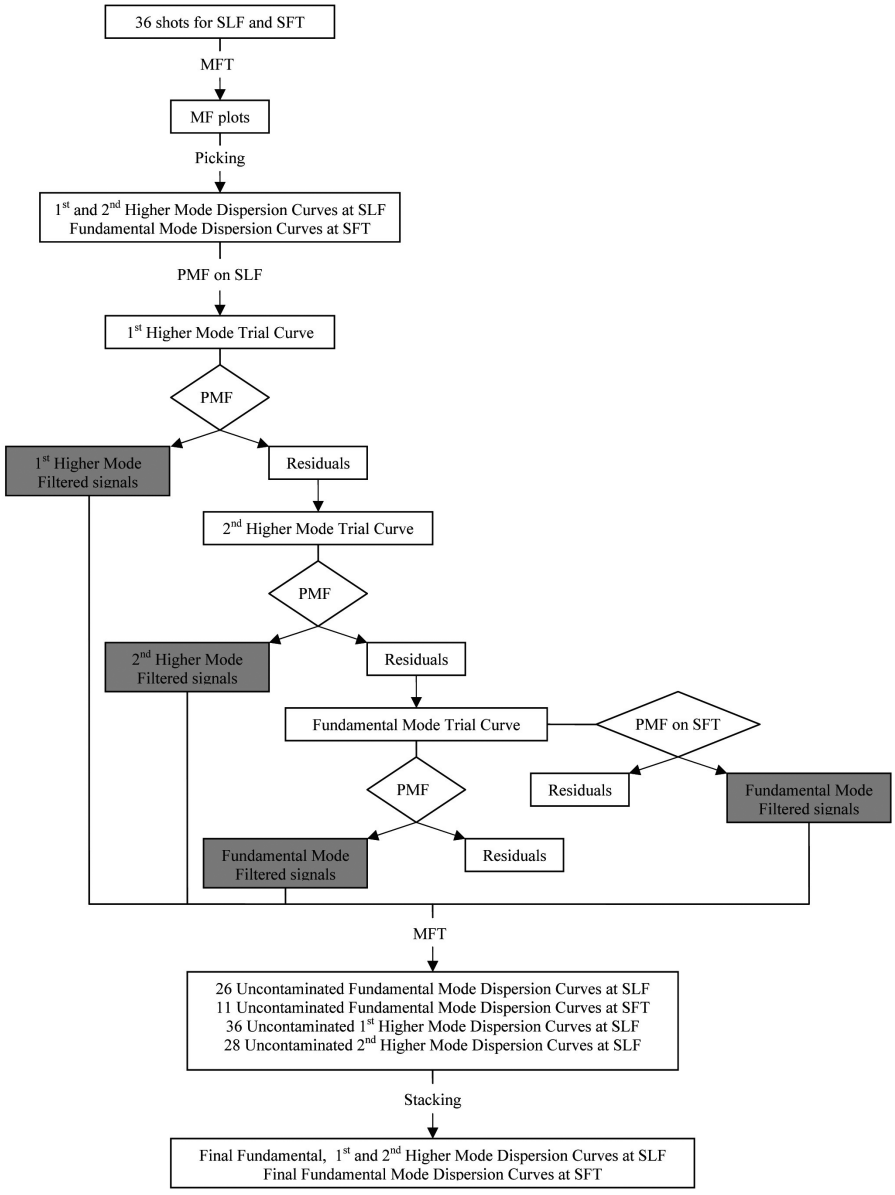

Fig. 4 - Block diagram describing the procedure used for the surface wave dispersion analysis.

To validate the results obtained for the fundamental mode at station SLF, a further phase-matched filtering was performed by using the trial fundamental dispersion on the seismograms recorded by the SFT station, to extract the fundamental-mode wave-packet.

The MFT was applied once again to all the filtered signals (both for SLF and SFT stations). As the filtered signal contains a single-mode wave-packet, the MFT produces a plot where the dispersion curve relative to that mode is greatly enhanced with respect to the non-filtered signal. Finally, a more robust and reliable estimate of the final dispersion relations is achieved by performing the stacking of a certain number of selected curves. The whole procedure is synthesized in the block diagram in Fig. 4. As one can appreciate from the example in Fig. 5, representing the stacked fundamental mode dispersion for the SLF station, after the combined use of MFT-PMF the dispersive pattern is very clear and it is no longer affected by higher mode contamination.

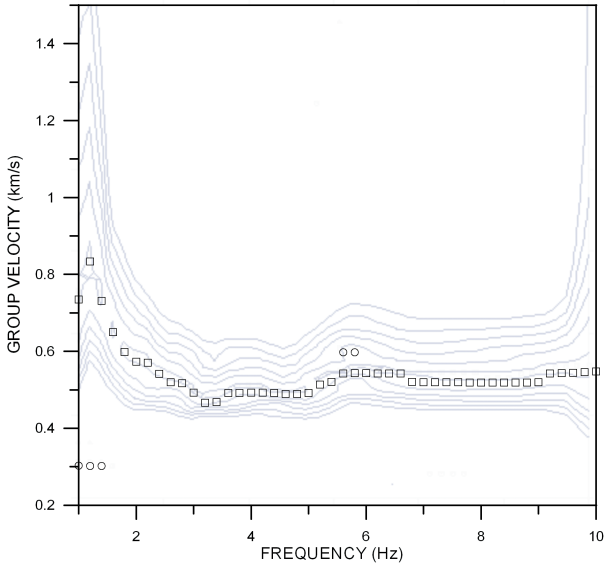

Fig. 5 - Stacked dispersion curve of the fundamental mode obtained after the application of PMF and MFT to data recorded at the SLF station.

The final dispersion relations for the fundamental, first and second mode are shown in Fig. 6. The comparison between the group velocity dispersion curves of the fundamental mode for stations SLF and SFT shows an excellent agreement of the two results.

To complete our study, we also performed an MFT analysis on POZ station, which is located near the coastline of Pozzuoli. No significant dispersive features were observed in the MF plots obtained for this data set. This means that the propagation in the water does not affect the dispersive pattern observed at the inner stations SFT and SLF, which is only due to the propagation of Rayleigh waves in a layered medium encompassed between the coast of Pozzuoli and the Solfatara crater. In this sense, the group velocity dispersion is representative of the average properties of the medium along this path.

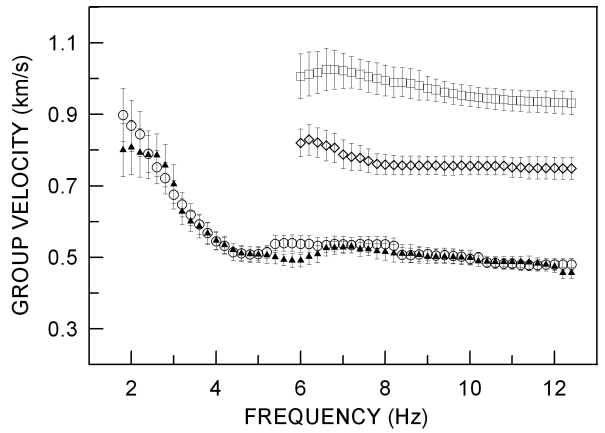

Fig. 6 - Stacked dispersion curves obtained from the application of MFT and PMF to data recorded at the SLF station for the fundamental (circle), first (diamond) and second (square) mode. Fundamental mode dispersion (triangle) for data recorded at the SFT station is also shown.

Inversion

The dispersion curves were inverted for a plane-layered Earth structure to infer the shallow shear-wave velocity model for the Pozzuoli-Solfatara area. Based on the available geological and geophysical observations, we build up a set of possible starting models with a variable number of layers (from the simple single-layer-models to 5-layer-models) and different S-wave velocities (chosen in the range 200-1500 m/s, which is compatible with the S-velocities typically observed for shallow soils and rocks in volcanic areas). Constraints for the minimum and maximum resolvable layer thickness and depths were imposed on the basis of the empirical relationships (Midzi, 2001). For the frequency range we investigated, the minimum resolvable layer thickness is in the order of 20 m, and the maximum resolvable depth is in the order of 250 m. We performed a first selection of the velocity structure by using a trial-and-error procedure to look for models which produced theoretical dispersion curves compatible with those experimentally observed. On this basis, some of the initial starting models with large misfits between observed and predicted data were rejected, while others were modified, adjusting layer thicknesses and velocities to better reproduce the dispersive pattern. The new subset of starting models was then inverted both for velocities and layer thicknesses by using the iterative procedure based on the computer code SURF (Herrmann, 1987). Some of these starting models as well as the corresponding models inferred by inversion are shown in Fig. 7. After the iterative inversion of the whole new subset, we selected the 3-layer-model because it yields the lowest rms value between observed and theoretical data and it fitted the greatest number of observations.

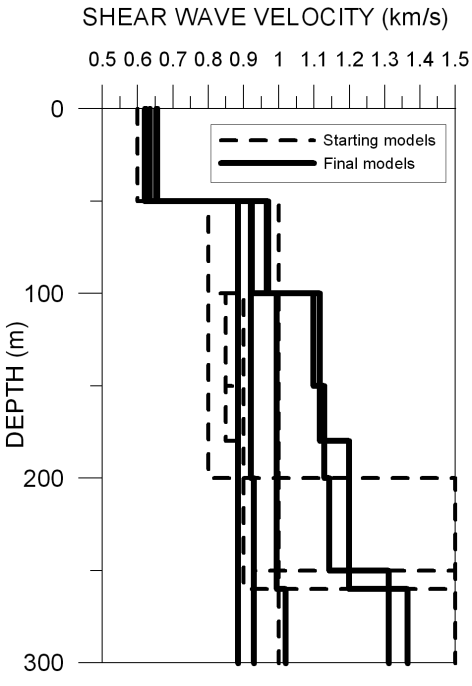

Fig. 7 - Some selected models used as trial velocity structure and the corresponding final models inferred from the inversion.

The three dispersion curves for the fundamental, first and second higher mode were inverted both separately and simultaneously to better constrain the results. All the inversions yield similar velocity models and stable results, and their robustness is evidenced by the fit between experimental and theoretical dispersions (Fig. 8). The inferred velocity models (Fig. 9) show a marked discontinuity at a depth of about 50 m where the shear-wave velocity abruptly changes from about 650 m/s to 900 m/s. Another slight increase of the S-velocity (from 900 m/s to 1000 m/s) is observed at a depth of about 100 m.

To verify how well these two discontinuities are constrained and to check the stability of the results obtained we perturbed the starting 3-layer model by changing both velocities and layer thicknesses and repeating the inversion procedure. In all the cases, the inversion converged to the final model previously described.

From the comparison of the resolution kernels, relative to the single and simultaneous inversions, we inferred that the last one provides the best

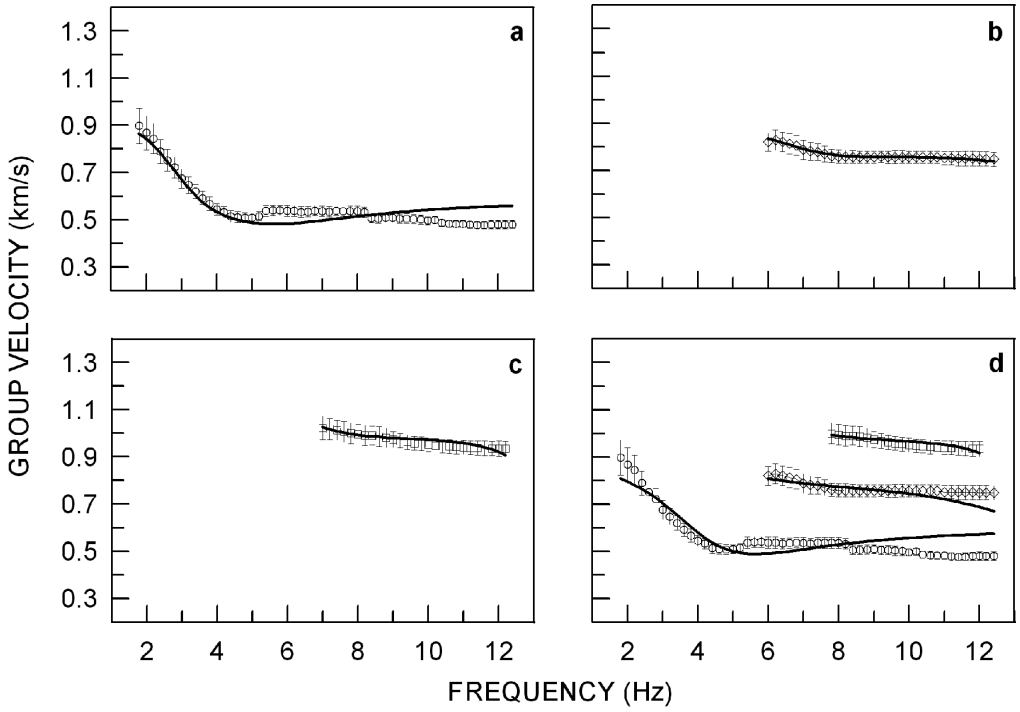

Fig. 8 - Results of fundamental (a), first (b), second higher mode (c), and simultaneous inversion of dispersion curves (d). The solid lines superimposed on the experimental data represent the theoretical dispersions obtained from the inferred shear-wave velocity model.

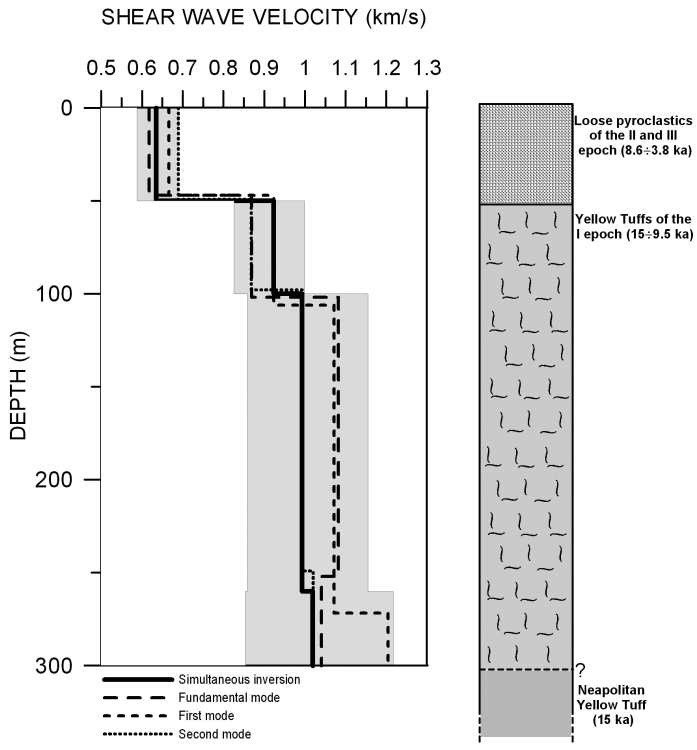

Fig. 9 - On the left, shear-wave velocity models obtained from single-mode and simultaneous inversions. The grey-shaded area represents the 2σ- uncertainty region associated to the velocity estimates. On the right, the possible geological interpretation of the velocity structure.

constrained velocity structure (because it yields the maximum resolution at different depths), hence, we use this model (hereinafter referred to as model A) for the error analysis. The uncertainties that affect this model are estimated by determining the range of shear-wave velocities obtained by the inversion procedure, when one considers the errors associated to the group velocity measurements. In fact, the stacked group velocity values calculated by the MFT are affected by uncertainties which are quantified in terms of the standard deviation σ. By subtracting and adding 2σ to the group velocity values, we generated the two extreme dispersion curves corresponding to the 95% error limits. These curves were then inverted to infer two extreme velocity models which actually represent the upper and lower bound for the model A. As one can note from Fig. 9, all the velocity models relative to both single-mode and simultaneous inversions are bounded by the 2σ error bars.

For a greater insight into our results, we compared the values retrieved for the shear-wave velocities with those derived in a previous study from cross- and down-hole measurements (Comune di Napoli, 1994). Although these data come from wells located in the western part of the city of Naples, they are associated with rocks formed after the NYT caldera eruption, so they can be considered indicative of the S-wave velocities for the volcanic products which characterize the area of Pozzuoli-Solfatara. For loose and unconsolidated ash deposits, the authors observed shear-wave velocities strongly depending on the depth and ranging from 180 m/s at depths of about 5 m to 800 m/s at a depth of 85 m, with a value of 550 m/s at a depth of about 50 m. For the compact tuff rocks (lithoid facies of NYT) typical Vs values are about 800-1000 m/s, with a weak dependence on depth.

From field and laboratory measurements Nunziata *et al*. (1999) evaluated the shear-wave velocities of the Phlegraean soils and tuffs, obtaining results in agreement with those reported above. Nunziata *et al*. (1999) found that for pyroclastic products and coastal deposits Vs is influenced by the increasing lithostatic pressure and ranges from 100 to 600 m/s over the 0-20 m depth range, while the compact NYT is characterized by Vs values ranging from 800 to 1100 m/s and weakly depending on the lithostatic load. Slightly lower shear-wave velocities are observed for fractured NYT but those values, unlike for the compact NYT, rapidly increase with pressure due to the closing of the fractures.

Velocity model interpretation

Taking into account the volcanological history, the geological constraints and comparison with literature data, we finally give a possible interpretation (Fig. 9) of the velocity model inferred from surface wave dispersion analysis. The first 50-m-thick layer could be composed of loose pyroclastic rocks emitted during the III epoch of activity and marine deposits of the La Starza terrace. The Vs value found for this layer is in fact compatible with those reported in the Comune di Napoli (1994) and Nunziata *et al*. (1999) for the same types of rocks. The seismic velocity discontinuity at 50 m can likely mark the transition to the yellow tuffs (which have analogous mechanical characteristics of NYT and hence similar shear-wave velocities) produced during the tuff-cone activity of the I epoch. The second discontinuity at 100-m-depth, which is less marked with respect to the shallower one, has two possible interpretations. It could be due to an effect of the lithostatic pressure which closes cracks and fractures in the tuff rock, with a consequent

increase of seismic velocity. Another possible explanation is that this discontinuity marks the contact between the products emitted by two distinct tuff cones which erupted during the I epoch. These units probably overlay the NYT bedrock. The interface with NYT is not resolved by our velocity model, whose maximum resolvable depth is of about 250 m. However, geological observations suggest a depth of about 300 m for the top of this unit (M. Di Vito, personal communication).

The velocity structure presented in this paper is in agreement with that recently obtained at a larger scale from a 3D seismic tomography by Vanorio *et al*. (2005), who observe low Vs values (1000-1200 m/s for the first 2 km) in the central part of the caldera. The present results are also compatible with the shallow velocity structure proposed for the Solfatara crater by Bruno *et al*. (2004). Although the model of Bruno *et al*. (2004) is limited to a depth of about 30 m, a rapid increase of Vs up to 540 m/s is reported for the lower bound of the structure.

Site response

The site response for the investigated area was estimated by computing the 1D theoretical transfer function. We considered a vertically-propagating shear-wave in the velocity structure previously described and estimated the theoretical response at the surface. Approximate damping values assigned to the different layers were derived from attenuation studies both in the Campi Flegrei and other volcanic areas (Del Pezzo *et al*., 1985; Petrosino *et al*., 2002). For a layered damped soil on an elastic bedrock the transfer function that relates the displacement amplitude at layer i to that of layer j can be calculated using the relation (Kramer, 1996):

$$F_{ij}(\omega) = \left| \frac{u_i}{u_j} \right| = \left| \frac{A_i(\omega) + B_i(\omega)}{A_j(\omega) + B_j(\omega)} \right|$$

with:

$$A_{m+1} = \frac{1}{2} A_m (1+\alpha_m^*) exp(ik_m^* h_m) + \frac{1}{2} B_m (1-\alpha_m^*) exp(-ik_m^* h_m)$$

$$B_{m+1} = \frac{1}{2} A_m (1-\alpha_m^*) exp(ik_m^* h_m) + \frac{1}{2} B_m (1+\alpha_m^*) exp(-ik_m^* h_m)$$

where h_m is the layer thickness, k_m^* is the complex wave number and α_m^* is the complex impedance contrast between the m-th and the (m+1)th layer. These last two parameters are defined through the complex shear wave velocity v^*:

$$k_m^* = \frac{2\pi f}{v_m^*} \qquad \alpha_m^* = \frac{\rho_m v_m^*}{\rho_{m+1} v_{m+1}^*} \qquad v_m^* = v_m \cdot (1 + i\xi_m)$$

with ρ_m and ξ_m density and damping of the m-th layer. The damping is related to the quality factor Q by the relation:

$$\xi = \frac{1}{2Q}$$

The parameters used to calculate the theoretical transfer function for the area of Pozzuoli-Solfatara are listed in Table 1:

Table 1 - Parameters to calculate the theoretical transfer function.

Layer number	Shear wave velocity (m/s)	Thickness (m)	Density (g/cm^3)	Quality factor
1 Loose pyroclastics	634	50	1.8	10
2 Fractured Yellow Tuff	923	50	1.9	20
Halfspace Compact Yellow Tuff	993	_	2.0	25

The transfer function obtained (Fig. 10) shows two peaks at a frequency of 2.2 and 5.4 Hz. The theoretical ground response derived for the Solfatara area should be considered indicative only of the resonance frequencies. Indeed, the amplification level needs to be better constrained by using more precise damping values for the soils and rocks characterizing the investigated area. In the future, these further constraints could be derived from both laboratory measurements and local attenuation studies aimed at determining the very shallow attenuation structure.

The theoretical transfer function was compared with the result obtained by applying Nakamura's technique (Nakamura, 1989) to microtremor data collected by the SLF station. To calculate the H/V spectral ratio, we selected 32 20-s-long time windows of seismic noise recorded between two consecutive air-gun shots. A Konno-Omachi smoothing window was applied to the Fourier spectra and, after the quadratic merging of the horizontal component, H/V spectral ratios were evaluated for each time window. Finally, these values were averaged to estimate the stacked H/V ratio for the site.

We also calculated the Nakamura spectral ratio using 21 artificial shots of the Serapis data set at the SLF station. In this case, we used a time window length of 10 s, while the other parameters set for the evaluation of the H/V spectral ratio were the same adopted for the noise analysis.

Finally, we also applied the method of Nakamura to 29 local earthquakes belonging to the seismic swarm that occurred in the area of the Solfatara on October 5, 2005. In this case, we used the seismic traces recorded at the SFT station because the SLF station was removed at the end of the Serapis experiment. In handling earthquake data, we selected a 5-s-long time window starting from the S-wave arrival, in order to analyse the contribution of the shear wave packet. For the H/V ratio estimate, we adopted the procedure previously described for the seismic noise.

As one can note in Fig. 10 the 5.4 Hz resonance frequency is observed both in the theoretical transfer function and in all the H/V ratios. On the contrary, the theoretical and experimental curves do not agree for the fundamental resonance frequency of 2.2 Hz which is observed only in the theoretical transfer function. The most probable hypothesis for this discrepancy is that the H/V ratio is sensitive to the velocity structure just beneath the station, while the 1D velocity model obtained from the inversion of Rayleigh wave dispersion represents an average model for the medium between the source and the receiver. So we expect that the H/V is compatible with

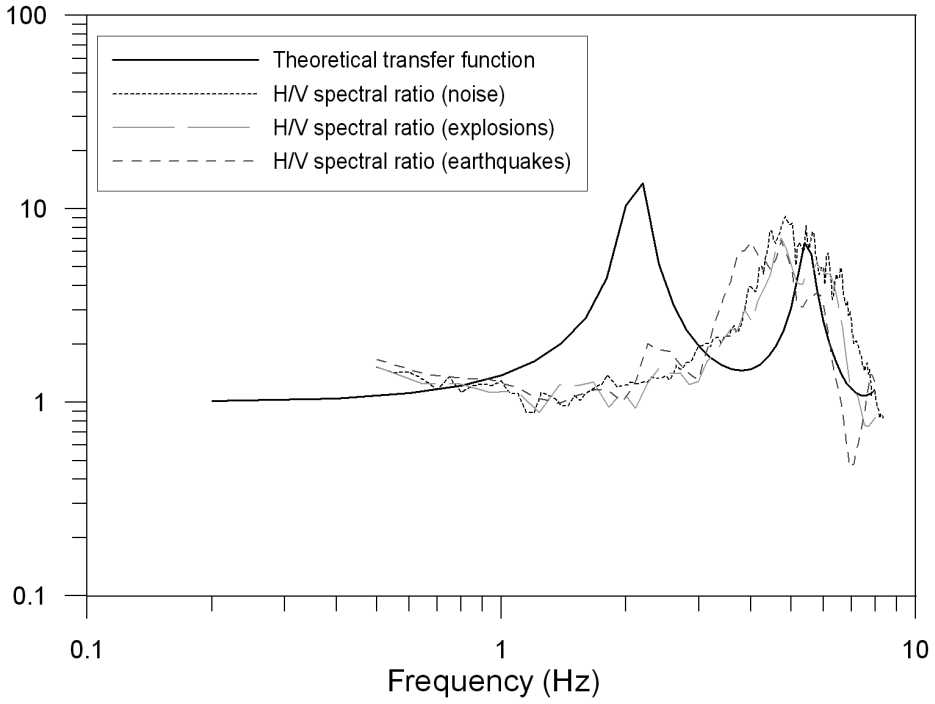

Fig. 10 - Theoretical transfer function calculated by using the inferred shear-wave velocity model and H/V spectral ratios obtained from the application of Nakamura's technique to microtremor, artificial explosions and local earthquakes.

the transfer function only for the case of a laterally-homogeneous structure. However, marked lateral velocity contrasts are expected as one moves from the inner part of the Solfatara crater to the outer, older part of the volcanic structure. In this case the H/V is to be considered indicative of the very local transfer function just for the Solfatara crater, while the transfer function derived from Rayleigh wave dispersion is valid for the area that goes from the shore of Pozzuoli to the external rim of the Solfatara crater.

A secondary hypothesis for consideration is that, as confirmed by many studies (Luzon *et al*., 2001; Malischewsky and Scherbaum, 2004) Nakamura's technique gives a good estimate of the fundamental frequency only in the case of large impedance contrast (generally > 2.5), while it often fails once dealing with low impedance contrast. For the Solfatara, we estimate an impedance contrast of about 1.5; under such conditions the H/V spectral ratio could not fully represent the site transfer function.

Conclusions

In this study, we assessed the problem of evaluating the shallow S-wave velocity structure in a volcanic environment, using a combination of both natural and artificial sources.

The combined use of MFT and PMF techniques has provided robust and stable results, which

have been successfully validated against the available constraints given by the direct and indirect geophysical and geological measurements.

These results are taken as representing the area included between the Pozzuoli coast and the Solfarara crater. Punctual evaluation of the response function of this latter site has been calculated using Nakamura's technique. Discrepancy between the two different results is attributed to lateral variations in the velocity profiles in the inner Solfatara crater.

Overall, this study contributes to the S-wave velocity characterization of the shallow velocity structure that might be considered for assessing site effects in the densely-populated Pozzuoli-Solfatara volcanic area.

Acknowledgments. We wish to thank Mauro Di Vito who provided useful information about the volcanological history of the Campi Flegrei Caldera and greatly helped us in the geological interpretation of the velocity model. Danilo Galluzzo and Mario La Rocca are greatly acknowledged for their contribution to the field work and data management. Thanks are also due to Vincenzo Nisii for the many helpful discussions. The map in Fig. 1 was plotted using the GMT software package.

REFERENCES

Aki K.; 1957: *Space and time spectra of stationary stochastic waves, with special reference to microtremors*. Bull. Earthq. Res. Inst. Tokio Univ., **25**, 415-457.

Bard P.-Y. and M. Bouchon; 1980: *The seismic response of sediment-filled valleys. Part 1: The case of incident SH waves*. Bull. Seism. Soc. Am., **70**, 1263-1286.

Bettig B., Bard P.Y., Scherbaum F., Riepl J., Cotton F., Cornou C., Hatzfeld D.; 2001: *Analysis of dense array noise measurements using the modified spatial autocorrelation method (SPAC). Application to the Grenoble area*. Boll. Geof. Teor. Appl., **42**, 15-27.

Bruno P.P., Bais G., Chiodini G., Godio A., Costi F.; 2004: *Geophysical study of the shallow hydrothermal system at Solfatara (Campi Flegrei; Italy)*. J. Geophys. Res., (submitted).

Comune di Napoli; 1994: *Indagini geologiche per l'adeguamento del P.R.G. alla legge regionale 07.01.1983 n. 9 in difesa del territorio dal rischio sismico*. Indagini per l'applicazione della L.R. n. 9/83.

Del Pezzo E., De Natale G., Scarcella G., Zollo A.; 1985: *Qc of three-component seismograms of volcanic microearthquakes at Campi Flegrei volcanic area – Southern Italy*. Pure Appl. Geophys., **123**, 683-696.

Di Vito M.A., Isaia R., Orsi G., Southon J., de Vita S., D'Antonio M., Pappalardo L., Piochi M.; 1999: *Volcanism and deformation since 12,000 years at the Campi Flegrei caldera (Italy)*. J. Volcanol. Geotherm. Res., **91**, 221-246.

Dziewonski A., Bloch S., Landisman M.; 1969: *A technique for the analysis of transient seismic signanals*. Bull. Seism. Soc. Am., **59**, 427-444.

Herrin E. and Goforth T.; 1977: *Phase-matched filters: application to the study of Rayleigh waves*. Bull. Seism. Soc Am., **67**, 1259-1275.

Herrmann R.B.; 1973: *Some aspects of band-pass filtering of surface waves*. Bull. Seism. Soc. Am., **63**, 663-671.

Herrmann R.B.; 1987: *Computer Programs in Seismology. User's manual Vol. II-IV*. St. Louis University, Missouri.

Hough S.E., Borcherdt R.D., Friberg P.A., Busby R., Field E., Jacobs K.H.; 1990: *The role of sediment-induced amplification in the collapse of the Nimitz freeway during the October 17, 1989 Loma Prieta earthquake*. Nature, **344**, 853-855.

Kramer S.L.; 1996: *Geotechnical earthquake engineering*. Prentice Hall Inc., Upper Saddle River, New Jersey.

Lirer L., Pescatore T.S., Corbelli V., Di Vito M., Gattullo V., Romano A.; 1987: *Geologia delle aree di Monteruscello e del centro storico di Pozzuoli*. Quaderno di documentazione n.1, Ministero della Protezione Civile, Napoli.

Louie J.N.; 2001: *Faster, better: shear-wave velocity to 100 meters depth from refraction microtremor arrays*. Bull. Seism. Soc. Am., **91**, 347-364.

Luzon F., Al Yuncha Z., Sanchez-Sesma F.J., Ortiz-Aleman C.; 2001: *A numerical experiment on the horizontal to vertical spectral ratio in flat sedimentary basins*. Pure Appl. Geophys., **158**, 2451-2461.

Malagnini L., Herrmann R.B., Biella G., de Franco R.; 1995: *Rayleigh waves in Quaternary alluvium from esplosive sources: determination of shear-wave velocity and Q structure*. Bull. Seism. Soc. Am., **85**, 900-922.

Malagnini L., Tricarico P., Rovelli A., Herrmann R.B., Opice S., Biella G., de Franco R.; 1996: *Explosion, earthquake, and ambient noise recordings in a pliocene sediment-filled valley: inferences on seismic response properties by reference- and non-reference-site techniques*. Bull. Seism. Soc. Am., **86**, 670-682.

Malischewsky P.G. and Scherbaum F.; 2004: *Love's formula and H/V-ratio (ellipticity) of Rayleigh waves*. Wave Motion, **40**, 57-67.

Midzi V.; 2001: *3-D surface wave group velocity distribution in Central-Southern Africa*. J. Seismology, **5**, 559-574.

Nakamura Y.; 1989: *A method for dynamic characteristics estimation of subsurface using microtremor on the ground surface*. Q. Rept. Railway Tech. Res. Inst., **30**, 1, 25-33.

Nunziata C., Mele R., Natale M.; 1999: *Shear wave velocities and primary influencing factors of Campi Flegrei-Neapolitan deposits*. Engineering Geology, **54**, 299-312.

Orsi G., De Vita S., Di Vito M.A.; 1996: *The restless resurgent Campi Flegrei nested caldera (Italy): constraints on its evolution and configuration*. J. Volcanol. Geotherm. Res., **74**, 179-214.

Orsi G., de Vita S., Di Vito M., Isaia R., Nave R., Heiken G.; 2003: *Facing volcanic and related hazards in the Neapolitan area*. In: Heiken G., Fakundiny R, Sutter J. (eds), Earth Sciences in Cities, American Geophysical Union book, Washington, **56**, 121-170.

Petrosino S., Cusano P., Saccorotti G., Del Pezzo E.; 2002: *Seismic attenuation and shallow velocity structures at Stromboli Volcano, Italy*. Bull. Seism. Soc. Am., **92**, 1102-1116.

Saccorotti G., Chouet B., Dawson P.; 2003: *Shallow-velocity models at the Kilauea Volcano, Hawaii, determined from array analyses of tremor wavefields*. Geophys. J. Int., **152**, 633-648.

Vanorio T., Virieux J., Zollo A., Capuano P., Russo G.; 2005: *3-D seismic tomography from P- and S- microearthquake traveltimes and rock physics characterization in the Campi Flegrei caldera*. J. Geophys. Res., 110, B03201, doi:10.1029/2004JB003102.

Zollo A., Judenherc S., Auger E., D'Auria L., Virieux J., Capuano P., Chiarabba C., de Franco R., Makris J., Michelini A., Musacchio G.; 2003: *Evidence for the buried rim of Campi Flegrei caldera from 3-d active seismic imaging.* Geophys. Res. Lett., 30(19), 2002, doi:10.1029/2003GL018173.

Corresponding author: Simona Petrosino
INGV - Osservatorio Vesuviano
Via Diocleziano, 328
80124 Napoli
e-mail: simona@ov.ingv.it